Supplemental Materials

Molecular Biology of the Cell

Cekan et al.

Supplemental Information

Supplemental Figure legends

Figure S1. **A computational model of the mitotic Ran system in HFF1 and HeLa cells.** (A) Schematic of the computational model of the minimal Ran system. RCC1 is restricted to the inner sphere that corresponds to the chromosomal volume, Ran is mobile throughout the cell, and all other components are exclusively localized in the cytoplasm (see Supplementary Text 1 and Supplementary Table 1 for details). (B) Schematic of the reactions included in the computational Ran system models. (C) Relative expression of the Ran system components in HeLa and HFF1 cells. Left, immunoblotting in total lysates of non-synchronized HeLa and HFF1 cells. Right, ratios of tubulin-normalized HFF1/HeLa levels for each protein (mean ± S.D, N=3). (D) Changes in average Ran·GTP levels in response to increasing RCC1 concentrations in HeLa or HFF1 fibroblast computational models. The saturating concentrations of RCC1 and its concentration at 40-fold increase are indicated. (E) FACS analyzes of asynchronous cultures of hTERT-RPE1WT and hTERT-RPE1RCC1V5 cells fixed and stained with propidium iodide (PI). The cell cycle phase composition is indicated.

Figure S2. Changes in Ran system during cell cycle arrest. (A) Changes in Ran system components in HFF1 cells exposed to replicative exhaustion (passage #30) or treated with doxorubicin, detected by immunoblotting. (B) The effects of doxorubicin treatment on the expression of RCC1 and TPX2 in normal fibroblasts (Wi-38 and CRL-1474) and HCT116 colorectal carcinoma cells.

Figure S3. SimpleWestern analysis of protein expression in cells recovering from doxorubicin-induced DNA damage. (A) Digital immunoblots (SimpleWestern) of total lysates of hTERT-RPE1^{WT} and hTERT-RPE1$^{RCC1\text{-}V5}$ cells untreated or treated with doxorubicin. Vinculin was used as a loading control. (B) Quantification of data shown in (A).

Figure S4. RCC1 overexpression overrides γ-irradiation- induced cell cycle arrest (A) Immunoblotting of total lysates from hTERT-RPE1^{WT} and hTERT-RPE1$^{RCC1\text{-}V5}$ cells recovering from γ-irradiation. (B) Column graph showing fractions of hTERT-RPE1^{WT} and hTERT-RPE1$^{RCC1\text{-}V5}$ cells that contained the indicated numbers of 53BP1 foci per nucleus during recovery from γ-irradiation. Means ± SD from two independent experiments, adjusted P-values from 2-way ANOVA with Sidak's multiple comparison tests.

Figure S5. Analysis of HCT116 clones recovered from doxorubicin treatment. (A) FACS analyzes of fixed and propidium iodide-stained HCT116^{WT} cells and three single-cell-derived clones of HCT116^{WT} cells that recovered from doxorubicin treatment. The fractions of G1, S, and G2 cells are shown beneath the graphs. (B) Summary of the characteristics of untreated HCT116^{WT} cells and HCT116 clones recovered from doxorubicin (C) Immunoblots of increasing loads of total cell lysates from HCT116^{WT} cells and doxorubicin –recovered HCT116 clones (D) Cell number in cultures of untreated HCT116^{WT} cells and doxorubicin recovered HCT116 clones. Means ± SD from two experiments performed in triplicates were fitted with exponential growth equations (dashed lines). (E) Graph of the population-doubling time and the relative

average RCC1 concentration in HCT116^{WT} cells and the single-cell-derived clones recovered from doxorubicin.

Figure S6. Microarray data on RCC1 expression in normal and tumor tissues.

Scatter plots of RCC1 mRNA expression detected by microarray analyzes in normal and tumor tissues in ovarian (Scotto *et al.*, 2008), colorectal (Alhopuro *et al.*, 2012) and carboplatin-resistant cervical tumors (Peters *et al.*, 2005). The GEO dataset accession numbers are indicated beneath the graphs.

Supplemental Text 1

Computational model of the minimal mitotic Ran system

We modeled the mitotic Ran▪GTP in HeLa- and HFF1-like cells using a reaction-diffusion model similar to numerical simulations developed previously (Gorlich *et al.*, 2003; Caudron *et al.*, 2005). The calculation was performed using a partial differential equation solver, pdepe, in Matlab and running the simulation until a steady-state was reached. The diffusion coefficients of proteins and the kinetic parameters, as well as protein concentrations for HeLa-like cells, were taken directly from previously described models (Caudron *et al.*, 2005; Kalab *et al.*, 2006). The protein concentrations for HFF1-like cells were estimated from the quantitative Western blot, and by adjusting for the difference in the cell volume between HeLa and HFF1 cells. The cell radius was estimated from measured cell volumes assuming that the cell is spherical, and the chromosome mass-radius is from fluorescence images of DAPI-stained mitotic cells. No parameters in the model were adjusted to fit the experimental results.

Supplemental Table 1.

Parameters of the computational mitotic Ran system models

Protein/Nucleotide	**HFF1 (μM)**	**HeLa (μM)**
Ran	3.1	6.0
RCC1	0.054	0.25
RanGAP1	0.28	0.4
RanBP1	0.68	1.1
Importin β	1.1	3.0
Cargo (SAF)	6.86	8.0
GTP	468	468
GDP	4.5	4.5

Protein species	**Localization**	**D ($\mu m^2/s$)**
Ran·GTP	Nuclear/cytoplasmic	22.0
RanGDP	Nuclear/cytoplasmic	22.0
Importin β	Cytoplasmic	14.0
RanBP1	Cytoplasmic	21.4
Ran·GTP -RanBP1	Cytoplasmic	17.2
Ran·GTP - Importin β	Cytoplasmic	13.0
Ran·GTP -RanBP1-Importin β	Cytoplasmic	12.2
Cargo (SAF)	Cytoplasmic	13.9
Importin β-SAF	Cytoplasmic	11.1
RCC1	Nuclear, immobile	NA
RCC1-Ran·GTP	Nuclear, immobile	NA
RCC1-Ran	Nuclear, immobile	NA
RCC1-RanGDP	Nuclear, immobile	NA
RanGAP1	Cytoplasmic, immobile	NA

	HFF1 (μm)	**HeLa (μm)**
Cell radius	9.0	9.9
Chromosomal sphere radius	5.5	6.7

Kinetic parameters	**Value**
R_1	74.4 $\mu M^{-1} s^{-1}$
R_2	21.1 s^{-1}
R_3	0.65 $\mu M^{-1} s^{-1}$
R_4	55 s^{-1}
R_5	102 $\mu M^{-1} s^{-1}$
R_6	19 s^{-1}
R_7	11.4 $\mu M^{-1} s^{-1}$
R_8	55 s^{-1}
k_{cat1}	10.6 s^{-1}
k_{cat2}	10.8 s^{-1}
K_{M1}	0.7 μM
K_{M2}	0.1 μM
k_{on1}	0.3 $\mu M^{-1} s^{-1}$
k_{off1}	0.0004 s^{-1}
k_{on2}	0.45 s^{-1}
k_{off2}	0.00045 s^{-1}
k_{on3}	0.3 s^{-1}
k_{off3}	0.045 s^{-1}
k_{c1}	0.49 $\mu M^{-1} s^{-1}$
k_{c2}	0.017 s^{-1}
k_{c3}	0.096 $\mu M^{-1} s^{-1}$
k_{c4}	4.8×10^{-12} s^{-1}

Supplemental Table 2

Matlab codes for the mitotic Ran system in HFF1 and HeLa cells

Matlab code for HFF1

```
function [otptv] = ranhff

m = 2;

x=0:.1:9.0; %distance along r

t=0:0.5:100; %s, time


sol = pdepe(m,@pdex4pde,@pdex4ic,@pdex4bc,x,t);

u1 = sol(:,:,1);  % µM, Ran·GTP

u2 = sol(:,:,2);  % µM, RanGDP

u3 = sol(:,:,3);  % µM, Ran·GTP -RCC1

u4 = sol(:,:,4);  % µM, Ran-RCC1

u5 = sol(:,:,5);  % µM, RanGDP-RCC1

u6 = sol(:,:,6);  % µM, RCC1

u7 = sol(:,:,7);  % µM, RanBP1

u8 = sol(:,:,8);  % µM, RanBP1-Ran·GTP

u9 = sol(:,:,9);  % µM, Importin Beta-Ran·GTP

u10 = sol(:,:,10);  % µM, Importin Beta RanBP1-Ran·GTP

u11 = sol(:,:,11);  % µM, Importin Beta

u12 = sol(:,:,12);  % µM, Cargo

u13 = sol(:,:,13);  % µM, Importin Beta-Cargo


u14 = 4*pi*0.1*(linspace(0, 9.0, 91).^2);

otptv = sum(u1(201,:).* u14)/((4*pi*9.0^3)/3); %free Ran·GTP  concentration in uM


% --------------------------------------------------------------

function [c,f,s] = pdex4pde(x,t,u,DuDx);
```

```
rchro = 5.5; %um, radius of chromosomes

Dr = 22; %um2 s-1,  diffusion coefficient of Ran·GTP  and RanGDP


if x<=rchro

  r1 = 74.4; %uM-1 s-1

  r2 = 21.1; %s-1

  r3 = 0.65; % uM-1 s-1

  r4 = 55; %s-1

  r5 = 102; %uM-1 s-1

  r6 = 19; %s-1

  r7 = 11.4; % uM-1 s-1

  r8 = 55; %s-1

  kcat1 = 0;

  kcat2 = 0;

  kon1 = 0;

  koff1 = 0;

  kon2 = 0;

  koff2 = 0;

  kon3 = 0;

  koff3 = 0;

  Dp = 0;

  D1 = 0;

  D2 = 0;

  D3 = 0;

  Dib = 0;

  Dc = 0;

  Dbc = 0;

  kc1 = 0;

  kc2 = 0;

  kc3 = 0;

  kc4 = 0;
```

```
else
  r1 = 0;
  r2 = 0;
  r3 = 0;
  r4 = 0;
  r5 = 0;
  r6 = 0;
  r7 = 0;
  r8 = 0;
  kcat1 = 10.6; %s-1
  kcat2 = 10.8; %s-1
  kon1 = 0.3; %s-1
  koff1 = 0.0004; %s-1
  kon2 = 0.45; %uM-1 s-1
  koff2 = 0.00045; %s-1
  kon3 = 0.3; %uM-1 s-1
  koff3 = 0.045; %s-1
  Dp = 21.4; %um2 s-1, diffusion coefficient of RanBP1
  D1 = 17.2; %um2 s-1, diffusion coefficient of RanBP1-Ran·GTP
  D2 = 13; %um2 s-1, diffusion coefficient of Ran·GTP -Importin Beta
  D3 = 12.2; %um2 s-1, diffusion coefficient of RanBP1-Ran·GTP -Importin Beta
  Dib = 14; %um2 s-1, diffusion coefficient of Importin Beta
  Dc = 13.9; %um2 s-1, diffusion coefficient of Cargo
  Dbc = 11.1; %um2 s-1, diffusion coefficient of Importin Beta-Cargo
  kc1 = 0.49; %uM-1 s-1
  kc2 = 0.017; %s-1
  kc3 = 0.096; %uM-1 s-1
  kc4 = 4.8e-12; %uM-1 s-1
end

kM1 = 0.7; %uM
```

```
kM2 = 0.1; %uM

GTP = 468; %uM, total GTP
GDP = 4.5; %uM, total GDP
RanGAP = 0.34; %uM, RanGAP1 concentration in cytoplasm

c = [1; 1; 1; 1; 1; 1; 1; 1; 1; 1; 1; 1; 1];
f = [Dr; Dr; 0; 0; 0; 0; Dp; D1; D2; D3; Dib; Dc; Dbc] .* DuDx/1;
s = [r4*u(3)-r5*u(6)*u(1)-kon1*u(7)*u(1)+koff1*u(8)-kon2*u(11)*u(1)+koff2*u(9)-kcat1*RanGAP*u(1)/(kM1+u(1))-
kc3*u(1)*u(13)+kc4*u(9)*u(12);
    r8*u(5)-r1*u(6)*u(2)+kcat1*RanGAP*u(1)/(kM1+u(1))+kcat2*RanGAP*u(8)/(kM2+u(8));
    r3*GTP*u(4)+r5*u(6)*u(1)-(r4+r6)*u(3);
    r2*u(5)+r6*u(3)-(r7*GDP+r3*GTP)*u(4);
    r7*GDP*u(4)+r1*u(6)*u(2)-(r2+r8)*u(5);
    r4*u(3)+r8*u(5)-(r1*u(2)+r5*u(1))*u(6);
    -kon1*u(7)*u(1)+koff1*u(8)-kon3*u(7)*u(9)+kcat2*RanGAP*u(8)/(kM2+u(8));
    kon1*u(7)*u(1)-koff1*u(8)-kcat2*RanGAP*u(8)/(kM2+u(8))+koff3*u(10);
    kon2*u(11)*u(1)-koff2*u(9)-kon3*u(7)*u(9)+kc3*u(1)*u(13)-kc4*u(9)*u(12);
    kon3*u(7)*u(9)-koff3*u(10);
    koff2*u(9)-kon2*u(1)*u(11)+koff3*u(10)-kc1*u(11)*u(12)+kc2*u(13);
    -kc1*u(11)*u(12)+kc2*u(13)+kc3*u(13)*u(1)-kc4*u(9)*u(12);
    kc1*u(11)*u(12)-kc2*u(13)-kc3*u(13)*u(1)+kc4*u(9)*u(12);
];
% --------------------------------------------------------------
function u0 = pdex4ic(x);
rchro = 5.5; %um, chromosome radius
Rantot = 3.1; %uM, total Ran

if x <= rchro
  RCC1tot = 0.24; %uM, total RCC1
  RanBP1tot = 0;
```

```
  ImportinBtot = 0;
  Cargotot = 0;
else
  RCC1tot = 0;
  RanBP1tot = 0.82; %uM, total RanBP1
  ImportinBtot = 1.3; %uM, total Importin Beta
  Cargotot = 8.3; %uM, total Cargo
end

u0 = [0; Rantot; 0; 0; 0; RCC1tot; RanBP1tot; 0; 0; 0; ImportinBtot; Cargotot; 0];  % uM, Initial conditions, initially,
concentrations of both species are 1 uM
% --------------------------------------------------------------
function [pl,ql,pr,qr] = pdex4bc(xl,ul,xr,ur,t)
pl = [0; 0; 0; 0; 0; 0; 0; 0; 0; 0; 0; 0; 0]; % constant term coefficient zero for left boundary
ql = [1; 1; 1; 1; 1; 1; 1; 1; 1; 1; 1; 1; 1];  % flux coefficients 1 for left boundary
pr = [0; 0; 0; 0; 0; 0; 0; 0; 0; 0; 0; 0; 0];  % constant term coefficients zero for right boundary
qr = [1; 1; 1; 1; 1; 1; 1; 1; 1; 1; 1; 1; 1];  % flux coefficients 1 for right boundary
```

Matlab code for HeLa

```
function [otptv] = ranhela
m = 2;
x=0:.1:9.9; %distance along r
t=0:0.5:100; %s, time

sol = pdepe(m,@pdex4pde,@pdex4ic,@pdex4bc,x,t);
u1 = sol(:,:,1);  % µM, Ran·GTP
u2 = sol(:,:,2);  % µM, RanGDP
u3 = sol(:,:,3);  % µM, Ran·GTP -RCC1
u4 = sol(:,:,4);  % µM, Ran-RCC1
```

```
u5 = sol(:,:,5);  % µM, RanGDP-RCC1

u6 = sol(:,:,6);  % µM, RCC1

u7 = sol(:,:,7);  % µM, RanBP1

u8 = sol(:,:,8);  % µM, RanBP1-Ran·GTP

u9 = sol(:,:,9);  % µM, Importin Beta-Ran·GTP

u10 = sol(:,:,10);  % µM, Importin Beta RanBP1-Ran·GTP

u11 = sol(:,:,11);  % µM, Importin Beta

u12 = sol(:,:,12);  % µM, Cargo

u13 = sol(:,:,13);  % µM, Importin Beta-Cargo


u14 = 4*pi*0.1*(linspace(0, 9.9, 100).^2);

otptv = sum(u1(201,:).* u14)/((4*pi*9.9^3)/3); %free Ran·GTP  concentration in uM



% ------------------------------------------------------------

function [c,f,s] = pdex4pde(x,t,u,DuDx);

rchro = 6.7; %um, radius of chromosomes

Dr = 22; %um2 s-1,  diffusion coefficient of Ran·GTP  and RanGDP


if x<=rchro

  r1 = 74.4; %uM-1 s-1

  r2 = 21.1; %s-1

  r3 = 0.65; % uM-1 s-1

  r4 = 55; %s-1

  r5 = 102; %uM-1 s-1

  r6 = 19; %s-1

  r7 = 11.4; % uM-1 s-1

  r8 = 55; %s-1

  kcat1 = 0;

  kcat2 = 0;

  kon1 = 0;
```

```
  koff1 = 0;
  kon2 = 0;
  koff2 = 0;
  kon3 = 0;
  koff3 = 0;
  Dp = 0;
  D1 = 0;
  D2 = 0;
  D3 = 0;
  Dib = 0;
  Dc = 0;
  Dbc = 0;
  kc1 = 0;
  kc2 = 0;
  kc3 = 0;
  kc4 = 0;
else
  r1 = 0;
  r2 = 0;
  r3 = 0;
  r4 = 0;
  r5 = 0;
  r6 = 0;
  r7 = 0;
  r8 = 0;
  kcat1 = 10.6; %s-1
  kcat2 = 10.8; %s-1
  kon1 = 0.3; %s-1
  koff1 = 0.0004; %s-1
  kon2 = 0.45; %uM-1 s-1
  koff2 = 0.00045; %s-1
```

```
  kon3 = 0.3; %uM-1 s-1
  koff3 = 0.045; %s-1
  Dp = 21.4; %um2 s-1, diffusion coefficient of RanBP1
  D1 = 17.2; %um2 s-1, diffusion coefficient of RanBP1-Ran·GTP
  D2 = 13; %um2 s-1, diffusion coefficient of Ran·GTP -Importin Beta
  D3 = 12.2; %um2 s-1, diffusion coefficient of RanBP1-Ran·GTP -Importin Beta
  Dib = 14; %um2 s-1, diffusion coefficient of Importin Beta
  Dc = 13.9; %um2 s-1, diffusion coefficient of Cargo
  Dbc = 11.1; %um2 s-1, diffusion coefficient of Importin Beta-Cargo
  kc1 = 0.49; %uM-1 s-1
  kc2 = 0.017; %s-1
  kc3 = 0.096; %uM-1 s-1
  kc4 = 4.8e-12; %uM-1 s-1
end

kM1 = 0.7; %uM
kM2 = 0.1; %uM

GTP = 468; %uM, total GTP
GDP = 4.5; %uM, total GDP
RanGAP = 0.57; %uM, RanGAP1 concentration in cytoplasm

c = [1; 1; 1; 1; 1; 1; 1; 1; 1; 1; 1; 1; 1];
f = [Dr; Dr; 0; 0; 0; 0; Dp; D1; D2; D3; Dib; Dc; Dbc] .* DuDx/1;
s = [r4*u(3)-r5*u(6)*u(1)-kon1*u(7)*u(1)+koff1*u(8)-kon2*u(11)*u(1)+koff2*u(9)-kcat1*RanGAP*u(1)/(kM1+u(1))-
kc3*u(1)*u(13)+kc4*u(9)*u(12);
    r8*u(5)-r1*u(6)*u(2)+kcat1*RanGAP*u(1)/(kM1+u(1))+kcat2*RanGAP*u(8)/(kM2+u(8));
    r3*GTP*u(4)+r5*u(6)*u(1)-(r4+r6)*u(3);
    r2*u(5)+r6*u(3)-(r7*GDP+r3*GTP)*u(4);
    r7*GDP*u(4)+r1*u(6)*u(2)-(r2+r8)*u(5);
    r4*u(3)+r8*u(5)-(r1*u(2)+r5*u(1))*u(6);
```

```
    -kon1*u(7)*u(1)+koff1*u(8)-kon3*u(7)*u(9)+kcat2*RanGAP*u(8)/(kM2+u(8));
    kon1*u(7)*u(1)-koff1*u(8)-kcat2*RanGAP*u(8)/(kM2+u(8))+koff3*u(10);
    kon2*u(11)*u(1)-koff2*u(9)-kon3*u(7)*u(9)+kc3*u(1)*u(13)-kc4*u(9)*u(12);
    kon3*u(7)*u(9)-koff3*u(10);
    koff2*u(9)-kon2*u(1)*u(11)+koff3*u(10)-kc1*u(11)*u(12)+kc2*u(13);
    -kc1*u(11)*u(12)+kc2*u(13)+kc3*u(13)*u(1)-kc4*u(9)*u(12);
    kc1*u(11)*u(12)-kc2*u(13)-kc3*u(13)*u(1)+kc4*u(9)*u(12);
];
% --------------------------------------------------------------
function u0 = pdex4ic(x)

rchro = 6.7; %um, chromosome radius
Rantot = 6; %uM, total Ran
if x <= rchro
  RCC1tot = 0.82; %uM, total RCC1
  RanBP1tot = 0;
  ImportinBtot = 0;
  Cargotot = 0;
else
  RCC1tot = 0;
  RanBP1tot = 1.6; %uM, total RanBP1
  ImportinBtot = 4.3; %uM, total Importin Beta
  Cargotot = 11.5; %uM, total Cargo
end

u0 = [0; Rantot; 0; 0; 0; RCC1tot; RanBP1tot; 0; 0; 0; ImportinBtot; Cargotot; 0];  % uM, Initial conditions, initially,
concentrations of both species are 1 uM
% --------------------------------------------------------------
function [pl,ql,pr,qr] = pdex4bc(xl,ul,xr,ur,t)
pl = [0; 0; 0; 0; 0; 0; 0; 0; 0; 0; 0; 0; 0]; % constant term coefficient zero for left boundary
ql = [1; 1; 1; 1; 1; 1; 1; 1; 1; 1; 1; 1; 1];  % flux coefficients 1 for left boundary
```

```
pr = [0; 0; 0; 0; 0; 0; 0; 0; 0; 0; 0; 0; 0];  % constant term coefficients zero for right boundary

qr = [1; 1; 1; 1; 1; 1; 1; 1; 1; 1; 1; 1; 1];  % flux coefficients 1 for right boundary
```

Supplemental References

Alhopuro, P., Sammalkorpi, H., Niittymaki, I., Bistrom, M., Raitila, A., Saharinen, J., Nousiainen, K., Lehtonen, H.J., Heliovaara, E., Puhakka, J., Tuupanen, S., Sousa, S., Seruca, R., Ferreira, A.M., Hofstra, R.M., Mecklin, J.P., Jarvinen, H., Ristimaki, A., Orntoft, T.F., Hautaniemi, S., Arango, D., Karhu, A., and Aaltonen, L.A. (2012). Candidate driver genes in microsatellite-unstable colorectal cancer. Int J Cancer *130*, 1558-1566.

Caudron, M., Bunt, G., Bastiaens, P., and Karsenti, E. (2005). Spatial coordination of spindle assembly by chromosome-mediated signaling gradients. Science *309*, 1373-1376.

Gorlich, D., Seewald, M.J., and Ribbeck, K. (2003). Characterization of Ran-driven cargo transport and the RanGTPase system by kinetic measurements and computer simulation. The EMBO Journal *22*, 1088-1100.

Kalab, P., Pralle, A., Isacoff, E.Y., Heald, R., and Weis, K. (2006). Analysis of a RanGTP-regulated gradient in mitotic somatic cells. Nature *440*, 697-701.

Peters, D., Freund, J., and Ochs, R.L. (2005). Genome-wide transcriptional analysis of carboplatin response in chemosensitive and chemoresistant ovarian cancer cells. Mol Cancer Ther *4*, 1605-1616.

Scotto, L., Narayan, G., Nandula, S.V., Arias-Pulido, H., Subramaniyam, S., Schneider, A., Kaufmann, A.M., Wright, J.D., Pothuri, B., Mansukhani, M., and Murty, V.V. (2008). Identification of copy number gain and overexpressed genes on chromosome arm 20q by an integrative genomic approach in cervical cancer: potential role in progression. Genes Chromosomes Cancer *47*, 755-765.

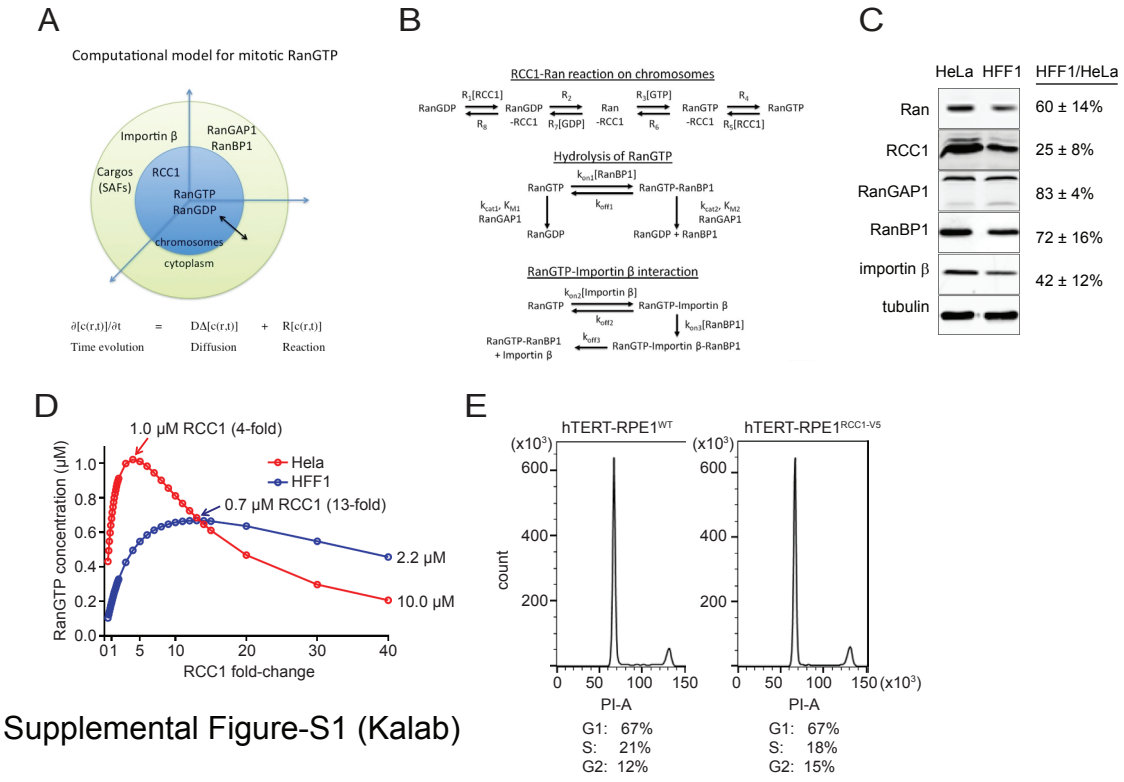

Supplemental Figure-S1 (Kalab)

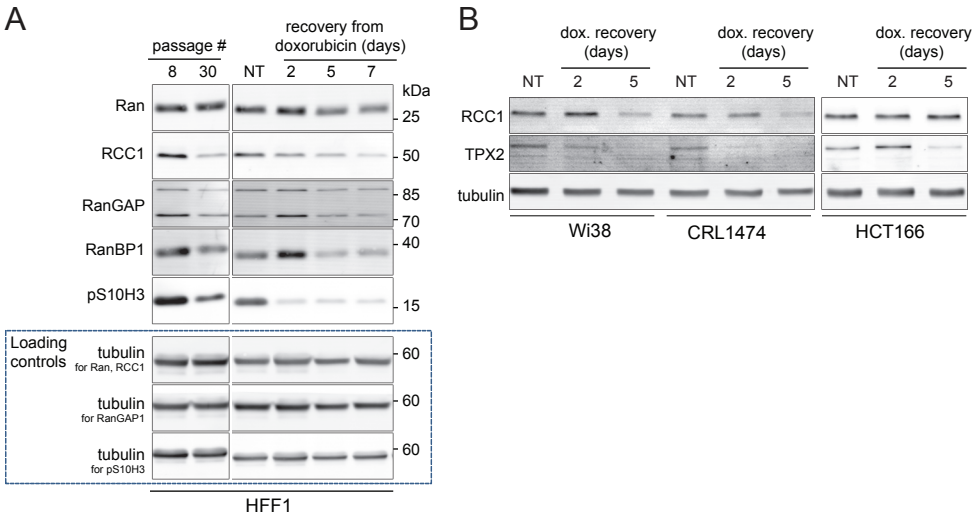

Supplemental Figure-S2 (Kalab)

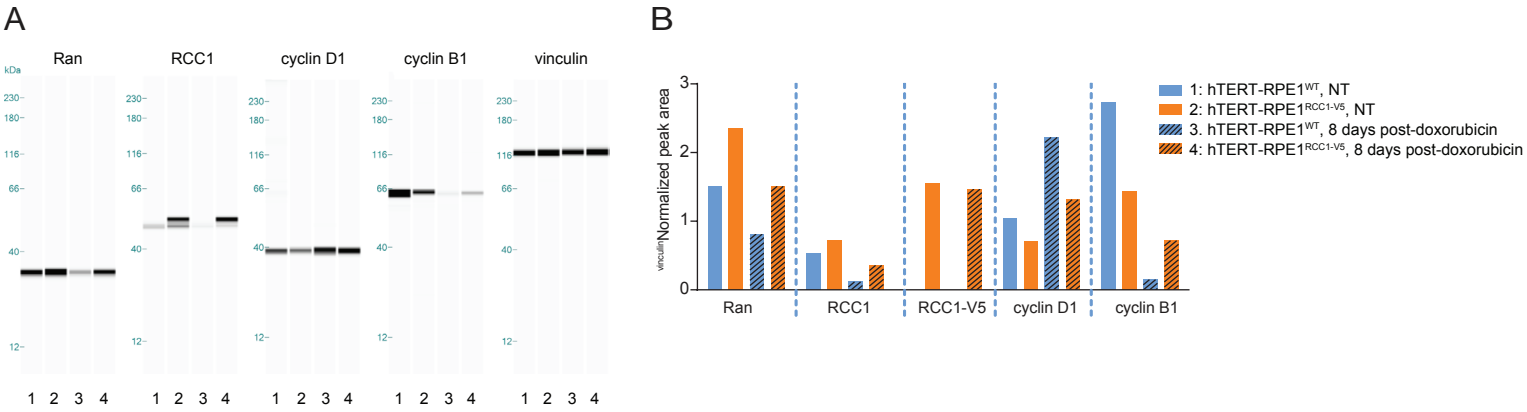

Supplemental Figure-S3 (Kalab)

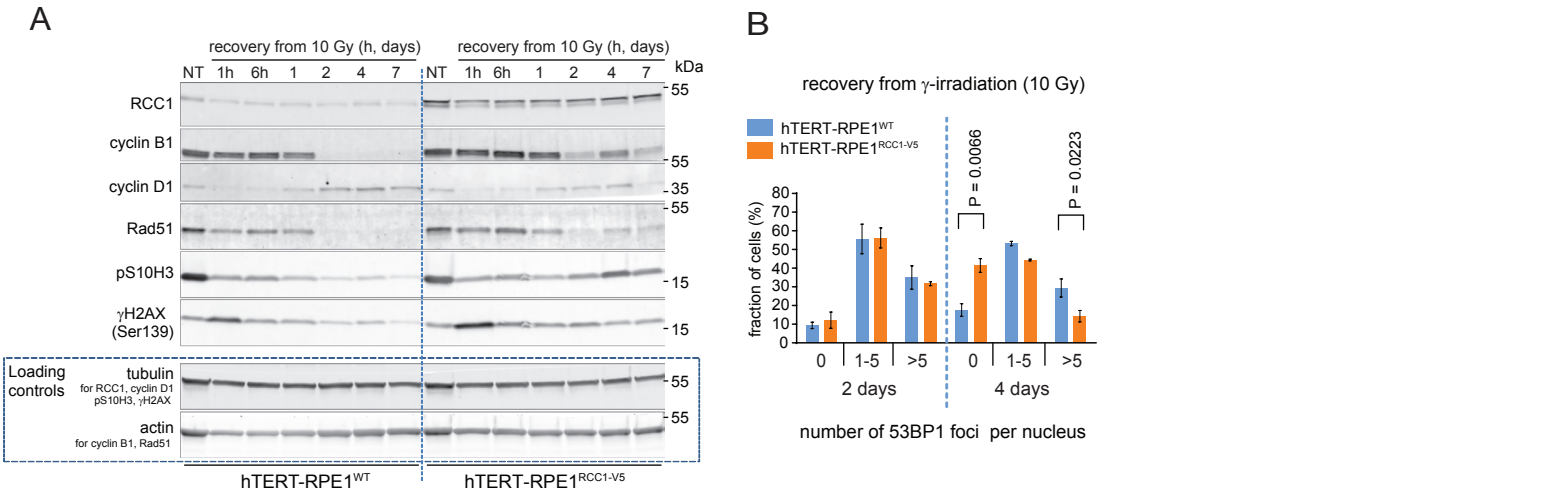

Supplemental Figure-S4 (Kalab)

A

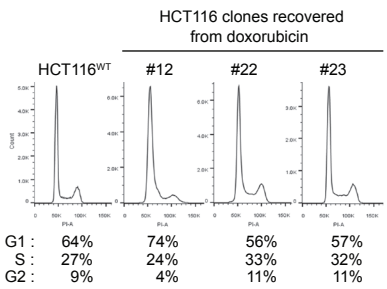

B

	pl cell volume (mean ± SD)	RCC1 WB signal/total cell lysate protein	RCC1 signal/cell volume (AU)	relative RCC1 signal/cell volume	population doubling (hours)
HCT116^{WT}	1.89±0.13	1.00	0.53	1.00	17.8
Clone #12	2.73±0.19	0.73	0.27	0.51	25.4
Clone #22	1.70±0.11	1.38	0.81	1.53	18.4
Clone #23	2.76±0.15	0.97	0.35	0.67	18.9

C

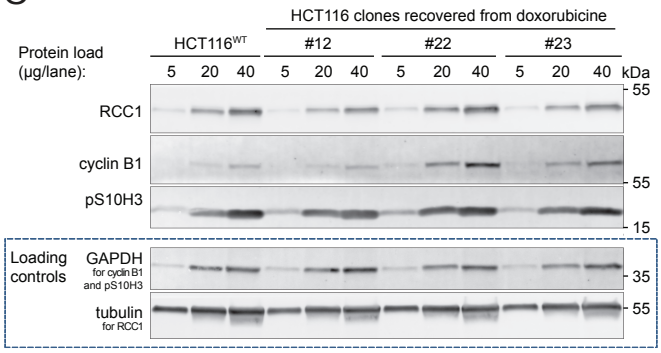

D

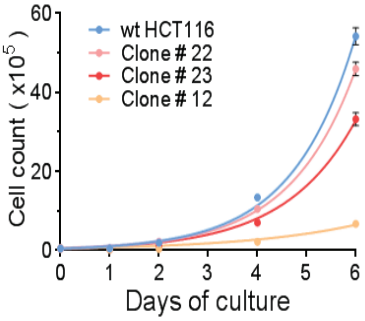

E

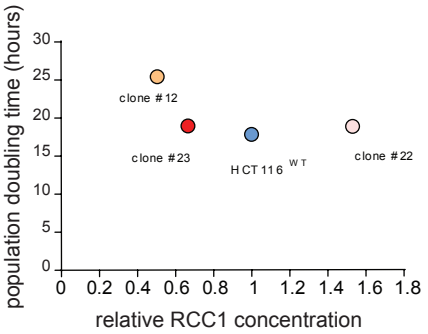

Supplemental Figure-S5 (Kalab)

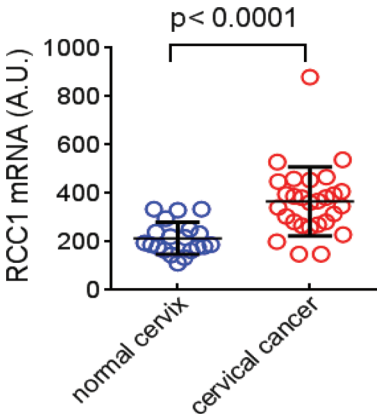

Cervical cancer (Scotto et al., 2008)
GEO Dataset: GDS3233

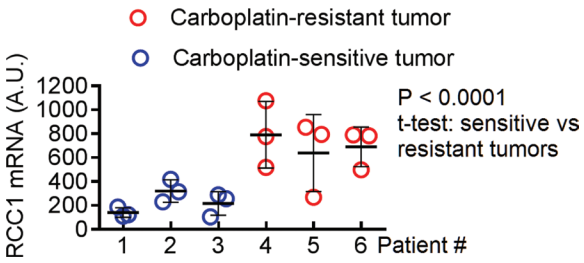

Ovarian cancer (Peters et al., 2005)
GEO Dataset: GDS1381

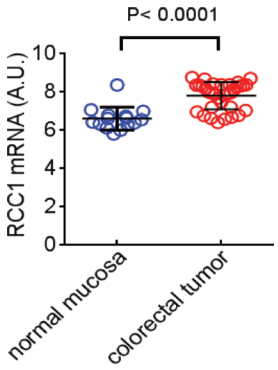

Colorectal cancer (Alhopuro et al., 2012)
GEO Dataset: GDS4515

Supplemental Figure-S6 (Kalab)